Dolichol-linked oligosaccharide selection by the oligosaccharyltransferase in protist and fungal organisms

Daniel J. Kelleher,[1] Sulagna Banerjee,[2] Anthony J. Cura,[1] John Samuelson,[2] and Reid Gilmore[1]

[1]Department of Biochemistry and Molecular Pharmacology, University of Massachusetts Medical School, Worcester, MA 01605
[2]Department of Molecular and Cell Biology, Goldman School of Dental Medicine, Boston University, Boston, MA 02118

The dolichol-linked oligosaccharide $Glc_3Man_9GlcNAc_2$-PP-Dol is the in vivo donor substrate synthesized by most eukaryotes for asparagine-linked glycosylation. However, many protist organisms assemble dolichol-linked oligosaccharides that lack glucose residues. We have compared donor substrate utilization by the oligosaccharyltransferase (OST) from *Trypanosoma cruzi*, *Entamoeba histolytica*, *Trichomonas vaginalis*, *Cryptococcus neoformans*, and *Saccharomyces cerevisiae* using structurally homogeneous dolichol-linked oligosaccharides as well as a heterogeneous dolichol-linked oligosaccharide library. Our results demonstrate that the OST from diverse organisms utilizes the in vivo oligosaccharide donor in preference to certain larger and/or smaller oligosaccharide donors. Steady-state enzyme kinetic experiments reveal that the binding affinity of the tripeptide acceptor for the protist OST complex is influenced by the structure of the oligosaccharide donor. This rudimentary donor substrate selection mechanism has been refined in fungi and vertebrate organisms by the addition of a second, regulatory dolichol-linked oligosaccharide binding site, the presence of which correlates with acquisition of the SWP1/ribophorin II subunit of the OST complex.

Introduction

The eukaryotic oligosaccharyltransferase (OST) transfers preassembled oligosaccharides onto asparagine residues as nascent polypeptides are translocated across the rough ER membrane (for review see Kelleher and Gilmore, 2006). The consensus site for N-linked glycosylation in eukaryotic organisms is conserved and corresponds to the simple tripeptide sequence N-X-T/S, where X can be any residue except proline (Gavel and Von Heijne, 1990).

The oligosaccharide donor assembled by most eukaryotes for N-linked glycosylation is the dolichol pyrophosphate–linked oligosaccharide $Glc_3Man_9GlcNAc_2$-PP-Dol (abbreviated here as $G_3M_9GN_2$-PP-Dol). Synthesis of the dolichol-linked oligosaccharide (OS-PP-Dol) donor occurs by the stepwise addition of monosaccharide residues onto the dolichol-pyrophosphate carrier by a family of ER-localized membrane bound glycosyltransferases (asparagine-linked glycosylation [ALG] gene products; for review see Burda and Aebi, 1999). $Man_5GlcNAc_2$-PP-Dol (M_5GN_2-PP-Dol) is assembled on the cytoplasmic face of the ER membrane, with UDP-GlcNAc and GDP-Man serving as monosaccharide donors. Man-P-Dol and Glc-P-Dol are the donors for the luminally oriented glycosyltransferases that add four mannose and three glucose residues to OS-PP-Dol assembly intermediates within the ER lumen. Depletion of the yeast Rft1 protein causes severe hypoglycosylation of proteins and accumulation of $Man_5GlcNAc_2$-PP-Dol (Helenius et al., 2002) even though Alg3p, not Rft1p, is the mannosyltransferase that adds the sixth mannose residue. Rft1p has been proposed to flip cytosolically oriented M_5GN_2-PP-Dol across the ER membrane (Helenius et al., 2002).

Certain kinetoplastids (*Trypanosoma cruzi* and *Leishmania mexicana*) and the ciliate *Tetrahymena pyriformis* assemble OS-PP-Dol compounds that lack the glucose residues (M_9GN_2-PP-Dol by *T. cruzi*) and/or the mannose residues ($G_3M_5GN_2$-PP-Dol by *T. pyriformis* and M_6GN_2-PP-Dol by *L. mexicana*) that are transferred by the luminally oriented ALG gene products (de la Canal and Parodi, 1987; Parodi, 1993). Searches of fully sequenced genomes using yeast ALG proteins as query sequences has revealed considerable diversity in OS-PP-Dol

Correspondence to Reid Gilmore: reid.gilmore@umassmed.edu

Abbreviations used in this paper: ALG, asparagine-linked glycosylation; HPLC, high-pressure liquid chromatography; OS-NYT, glycosylated tripeptide; OS-PP-Dol; dolichol-linked oligosaccharide; OST, oligosaccharyltransferase; PIC, protease inhibitor cocktail.

The online version of this article contains supplemental material.

The Journal of Cell Biology, Vol. 177, No. 1, April 9, 2007 29–37
http://www.jcb.org/cgi/doi/10.1083/jcb.200611079

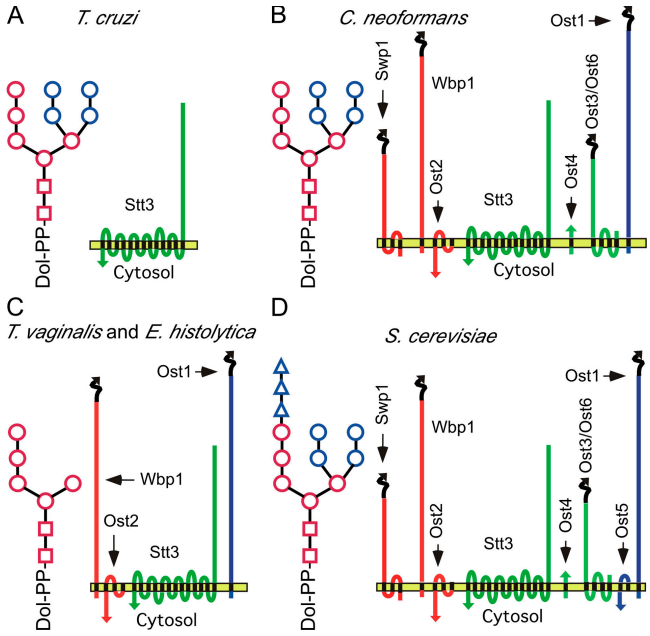

Figure 1. **OS-PP-Dol donors and predicted subunit compositions of the OST from selected eukaryotes.** The left portion of A–D shows the oligosaccharide structure of the in vivo donor for N-linked glycosylation. *N*-acetylglucosamine residues are designated by squares, mannose residues are shown as circles, and glucose residues are shown as triangles. Red saccharides are transferred by cytoplasmically oriented ALG gene products, and blue residues are transferred by luminally oriented ALG gene products. The right section of each panel shows the predicted (A, *T. cruzi*; B, *C. neoformans*; or C, *T. vaginalis* and *E. histolytica*) or experimentally determined (D, *S. cerevisiae*) composition of the OST complex. The color code of the subunits (red, green, and blue) designates subcomplexes detected in higher eukaryotes (Karaoglu et al., 1997; Spirig et al., 1997). The yellow bar designates the ER membrane.

biosynthesis amongst unicellular organisms (Samuelson et al., 2005). Biochemical studies have confirmed bioinformatic predictions that *Giardia lamblia* synthesizes GN_2-PP-Dol, *Trichomonas vaginalis* and *Entamoeba histolytica* synthesize M_5GN_2-PP-Dol, and the pathogenic fungi *Cryptococcus neoformans* synthesizes M_9GN_2-PP-Dol (Fig. 1; Samuelson et al., 2005). The diversity of eukaryotic OS- PP-Dol donors was proposed to have occurred by secondary loss of ALG genes during the evolution of current eukaryotes from a last common ancestor with a complete ALG pathway (Samuelson et al., 2005).

In fungi and vertebrate organisms, the OST is an oligomer composed of seven to eight nonidentical subunits (for review see Kelleher and Gilmore, 2006). Of the eight *Saccharomyces cerevisiae* OST subunits (Stt3p, Ost1p, Ost2p, Ost3p or Ost6p, Ost4p, Ost5p, Wbp1p, and Swp1p), five are encoded by essential yeast genes (*STT3*, *OST1*, *OST2*, *WBP1*, and *SWP1*). With the exception of STT3, which contains the enzyme active site (Yan and Lennarz, 2002; Kelleher et al., 2003; Nilsson et al., 2003), relatively little is known about the roles of the essential or nonessential subunits (for review see Kelleher and Gilmore, 2006). Vertebrate, plant, and insect genomes encode two forms of the catalytic subunit that are designated as STT3A and -B (Kelleher et al., 2003; Koiwa et al., 2003). The canine STT3 homologues are assembled with a shared set of noncatalytic subunits (ribophorin I [Ost1 homologue], ribophorin II [Swp1], OST48 [Wbp1], DAD1 [Ost2], and TUSC3 or IAP [Ost3 or -6] and OST4) to generate OST isoforms with kinetically distinct properties (Kelleher et al., 2003). Protein and DNA sequence database searches of fully sequenced eukaryotic genomes using the yeast and human OST subunits as query sequences suggest that the OST in protist organisms has a simpler subunit composition (Fig. 1; Kelleher and Gilmore, 2006). The genomes of *G. lamblia* and the kinetoplastids *T. cruzi* and *Trypanosoma brucei* encode several different STT3 proteins (Samuelson et al., 2005), yet lack genes encoding the noncatalytic subunits. Four-subunit complexes, consisting of STT3, OST1, OST2, and WBP1, are predicted for *T. vaginalis* and *E. histolytica*. A six-subunit complex (STT3, OST1, OST2, OST3, OST4, and WBP1) is predicted for *Cryptosporidium parvum*. The *C. neoformans* genome encodes readily identifiable homologues of all *S. cerevisiae* OST subunits with the exception of Ost5p (Fig. 1).

The absence of glucose residues on OS-PP-Dol compounds assembled by most protists and *C. neoformans* is of particular interest because the terminal glucose residue on $G_3M_9GN_2$-PP-Dol is a critical substrate recognition determinant for the OST. OS-PP-Dol assembly intermediates that lack the terminal glucose residue are transferred less rapidly by the vertebrate and yeast OST (Turco et al., 1977; Trimble et al., 1980; Bosch et al., 1988; Karaoglu et al., 2001; Kelleher et al., 2003), thereby minimizing synthesis of glycoproteins with aberrant oligosaccharide structures. Glycosylation of proteins with an oligosaccharide assembly intermediate could interfere with glycoprotein quality-control pathways in the ER as well as subsequent oligosaccharide-processing reactions in the Golgi complex (for review see Helenius and Aebi, 2004). Cellular defects in $G_3M_9GN_2$-PP-Dol biosynthesis cause a family of inherited diseases (congenital disorders of glycosylation [CDG-I]) due to hypoglycosylation of nascent glycoproteins by the OST in cells that accumulate an assembly intermediate or are unable to maintain a normal concentration of fully assembled $G_3M_9GN_2$-PP-Dol (for review see Freeze and Aebi, 2005).

Preferential utilization of $G_3M_9GN_2$-PP-Dol by the yeast and vertebrate OST occurs by allosteric interactions between a regulatory OS-PP-Dol binding site and the active site subunit, as well as by oligosaccharide structure–mediated alterations in tripeptide acceptor binding affinity (Karaoglu et al., 2001; Kelleher et al., 2003). Kinetic analysis of the purified canine OST isoforms has suggested that the regulatory OS-PP-Dol binding site is not located on STT3A or -B, but is instead associated with one or more of the noncatalytic subunits (Kelleher et al., 2003).

Does the OST from organisms that synthesize nonglucosylated OS-PP-Dols transfer the in vivo donor in preference to OS-PP-Dol assembly intermediates or $G_3M_9GN_2$-PP-Dol? Previous studies indicate that the *T. cruzi* OST transfers glucosylated ($G_{1\text{-}3}M_9GN_2$-PP-Dol) and large nonglucosylated ($M_{7\text{-}9}GN_2$-PP-Dol) donors at similar rates in vitro (Bosch et al., 1988), suggesting that the *T. cruzi* OST is nonselective. Can biochemical analysis of the OST from primitive eukaryotes reveal properties of the higher eukaryotic OST that arose as additional subunits were added to the STT3 catalytic core? Here, we report a comparison of the OST from *T. vaginalis*, *E. histolytica*, *T. cruzi*, *C. neoformans*, and *S. cerevisiae*, with emphasis placed upon an analysis of donor

substrate selection. Our results support the hypothesis that terminal mannose residues on the OS-PP-Dol are important for donor substrate recognition by the OST in organisms that assemble nonglucosylated OS-PP-Dol compounds. Cooperative OS-PP-Dol binding, a feature of the yeast and canine OST complex that facilitates exquisite $G_3M_9GN_2$-PP-Dol selection, is not a property of the predicted one- and four-subunit protist OST complexes.

Results

Donor substrate selection by the OST

Is preferential utilization of the in vivo oligosaccharide donor an OST property that is restricted to eukaryotes that assemble triglucosylated OS-PP-Dols? To address this question, the OST from selected protists and *C. neoformans* was assayed using a synthetic tripeptide acceptor and a heterogeneous bovine OS-PP-Dol library that consists of donors that range in size between M_3GN_2-PP-Dol and $G_3M_9GN_2$-PP-Dol. Enzyme concentrations were adjusted to ensure that a maximum of 3% of the total donor substrate was converted into glycopeptides. Radiolabeled glycopeptide products that were captured with an immobilized lectin (ConA Sepharose) were subsequently eluted and resolved by high-pressure liquid chromatography (HPLC) according to the number of saccharide residues (Fig. 2). As expected, $G_3M_9GN_2$-NYT was the most abundant product when the purified *S. cerevisiae* OST was assayed (Fig. 2 A). In contrast, $G_3M_9GN_2$-NYT was less abundant in the *T. cruzi* glycopeptide products (Fig. 2 B) and barely detectable in glycopeptide products derived from assays of the *T. vaginalis* (Fig. 2 C), *C. neoformans* (Fig. 2 D), or *E. histolytica* (not depicted) OST. The composition of the OS-PP-Dol donor library was determined as described previously (Kelleher et al., 2001) by incubating an excess of the purified yeast OST with a low quantity of the donor substrate (OST endpoint assay; Fig. S1, available at http://www.jcb.org/cgi/content/full/jcb.200611079/DC1). A normalized initial transfer rate (glycosylated tripeptide [OS-NYT]/OS-PP-Dol; Fig. 2, E and F) was calculated for the eight most abundant donors by dividing the glycopeptide product composition by the composition of the OS-PP-Dol donor substrate library. A normalized initial transfer rate of 1 (Fig. 2, E and F, dashed lines) indicates nonselective utilization of a donor substrate relative to the total donor pool.

The *T. vaginalis* and *E. histolytica* OST transfer the mannosylated donors ($M_{4\text{-}9}GN_2$-PP-Dol) threefold more rapidly than $G_3M_9GN_2$-PP-Dol (Fig. 2, E and F). Although the *T. cruzi* OST utilizes compounds ranging in size between M_7GN_2-PP-Dol and $G_3M_9GN_2$-PP-Dol at rates similar to those reported previously (Bosch et al., 1988), OS-PP-Dol donors with fewer mannose residues ($M_{3\text{-}6}GN_2$-PP-Dol) were transferred less rapidly (Fig. 2 F). The *C. neoformans* OST showed preferential utilization of the in vivo donor (M_9GN_2-PP-Dol) relative to assembly intermediates ($M_{3\text{-}6}GN_2$-PP-Dol) and the glucosylated donor (Fig. 2 F).

Structural determinants of donor substrate selection

Careful inspection of the glycopeptide elution profiles (Fig. 2, A–D) revealed that several of the smaller glycopeptide peaks

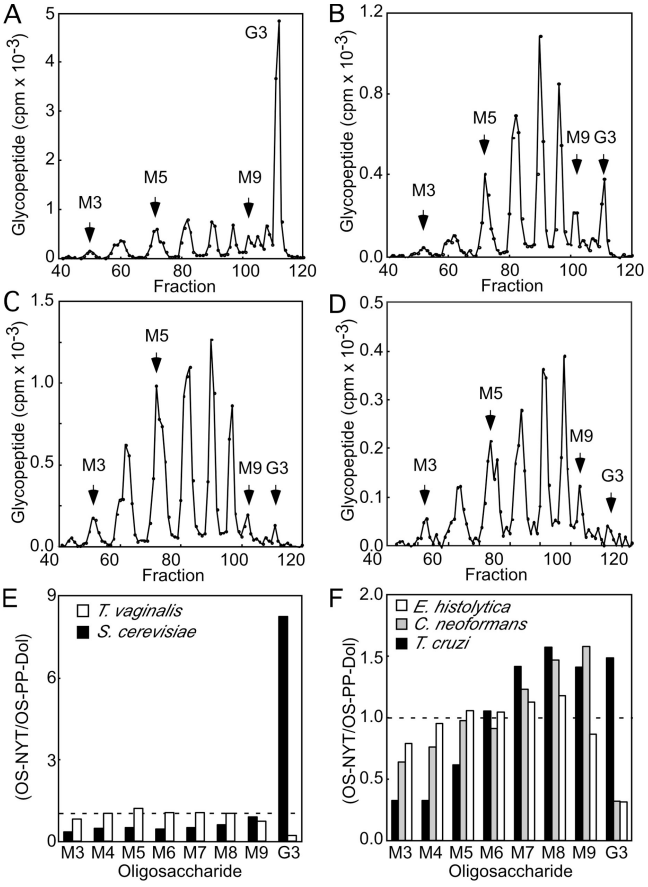

Figure 2. **Donor substrate selection from an OS-PP-Dol library.** The purified yeast OST (A) or detergent extracts prepared from *T. cruzi* (B), *T. vaginalis* (C), *C. neoformans* (D), or *E. histolytica* (not depicted) membranes were assayed for OST activity in the presence of glucosidase and mannosidase inhibitors using 1.2 μM OS-PP-Dol and 10 μM tripeptide acceptor (Nα-Ac-N-[^{125}I]-Y-T NH_2). Glycopeptide products ranging in size between M_3GN_2-NYT (M3) and $G_3M_9GN_2$-NYT (G3) were resolved by HPLC and identified by migration relative to authentic standards (M5, M9, and G3). (E and F) The normalized initial transfer rate (OS-NYT/OS-PP-Dol) for the eight most abundant OS-PP-Dol donors was calculated by dividing the composition of the glycopeptide products by the composition of the OS-PP-Dol donor library. The OST from all organisms was assayed twice to determine the composition of the product pool. The composition of the donor pool was determined by duplicate assays (Fig. S1, available at http://www.jcb.org/cgi/content/full/jcb.200611079/DC1). Note the difference in ordinate scales for E and F.

(e.g., M_5GN_2-NYT) have prominent shoulders, suggesting oligosaccharide structural heterogeneity. The structural diversity of the OS-PP-Dol donor substrate library is thought to arise by exposure of $G_3M_9GN_2$-PP-Dol to cellular glucosidases and mannosidases during isolation (Kelleher et al., 2001). Mannosidase degradation of M_9GN_2-PP-Dol (Fig. 3 A, compound a) could yield seven M_5GN_2-PP-Dol isomers (Fig. 3 A, compounds c–i) that differ from biosynthetic M_5GN_2-PP-Dol (Fig. 3 A, compound b). Biosynthetic M_5GN_2-PP-Dol (Fig. 3 A, compound b) can be readily distinguished from these other isomers by digestion with α-1,2 mannosidase, as it is the only isomer that has two α-1,2–linked mannose residues (Fig. 3 A, red circles). M_5GN_2 glycopeptides produced in an OST endpoint assay were purified by preparative HPLC (Fig. 3 B, left) and digested to completion with α-1,2 mannosidase. Resolution of

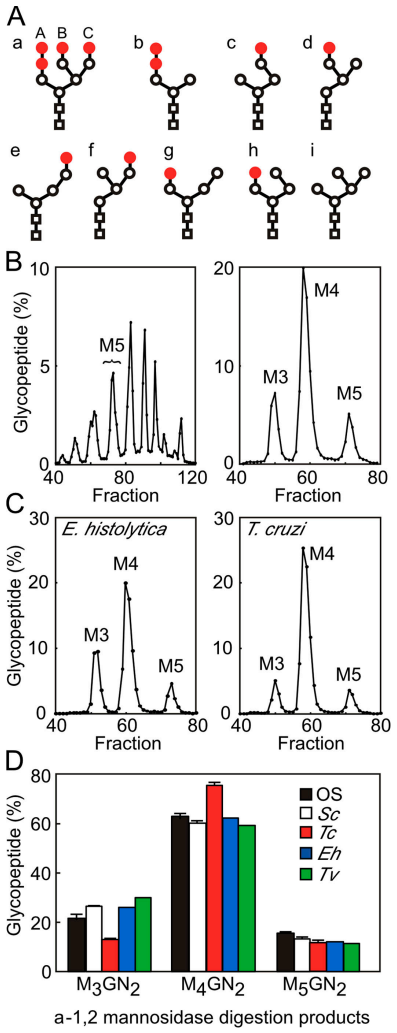

Figure 3. **Reduced transfer of biosynthetic M_5GN_2-PP-Dol by the *T. cruzi* OST.** (A) Biosynthetic M_5GN_2-PP-Dol (b) and M_5GN_2-PP-Dol isomers (c–i) produced by mannosidase digestion of M_9GN_2-PP-Dol (a). GlcNAc residues are indicated by squares, α-1,2–linked mannose residues are indicated by red circles, and α-1,3– and α-1,6–linked mannose residues are indicated by open circles. (B) Glycopeptide products obtained in an OST endpoint assay (>95% conversion of OS-PP-Dol to OS-NYT) were resolved by preparative HPLC to isolate the M_5GN_2-NYT glycopeptide (left). HPLC resolution of the α-1,2 mannosidase digestion products derived from M_5GN_2-NYT (right). The M_3GN_2-NYT (M3) peak is derived from isomer b, the M_4GN_2-NYT (M4) peak is derived from isomers c–h, and the M_5GN_2-NYT (M5) peak corresponds to isomer i. (C) HPLC profiles of α-1,2 mannosidase digestion products derived from M_5GN_2-NYT synthesized by the *E. histolytica* and *T. cruzi* OST. Redigestion of the M4 peak with α-1,2 mannosidase did not yield smaller products (not depicted); hence, the initial digestion had gone to completion. (D) The distribution of the three isomer classes (2, 1, or 0 α-1,2–linked mannose residues) was calculated for the total M_5GN_2-PP-Dol pool (OS) and for M_5GN_2-NYT synthesized by the *S. cerevisiae* (*Sc*), *T. cruzi* (*Tc*), *E. histolytica* (*Eh*), and *T. vaginalis* (*Tv*) OST. Values for the OS, *Sc*, and *Tc* are means of two independent experiments; error bars designate one of two independent data points. The OS values are derived from two replicates of B.

the digestion products by HPLC (Fig. 3 B, right) yielded three peaks (M3, M4, and M5) that are derived from M_5GN_2-PP-NYT isomers that contain 2, 1, or 0 α-1,2–linked mannose residues. Quantification (Fig. 3 D, black bars) of two independent experiments revealed that 22% of the M_5GN_2 glycopeptides were derived from biosynthetic M_5GN_2-PP-Dol (Fig. 3 A, compound b), 63% from compounds c–h, and 15% from compound i.

If the OST from *T. vaginalis*, *E. histolytica*, *T. cruzi*, or *S. cerevisiae* selects biosynthetic M_5GN_2-PP-Dol (Fig. 3 A, compound b) in preference to other M_5GN_2-PP-Dol isomers, the M_5GN_2 glycopeptides synthesized in the presence of excess donor substrate should be enriched in glycopeptides that contain two α-1,2–linked mannose residues. To ensure that our glycopeptide product analysis provided a reliable measure of the relative initial transfer rate, the OST assays were terminated when <10% of the total M_5GN_2-PP-Dol was converted into glycopeptides. Typical HPLC profiles of the α-1,2 mannosidase digestion products of the M_5GN_2 glycopeptides are shown in Fig. 3 C, and the results from assays of all four organisms are quantified in Fig. 3 D. We observed a very similar distribution of M_5GN_2 isomers for the donor substrate pool and the initial *S. cerevisiae* glycopeptide products (Fig. 3 D, compare black and white bars), thereby indicating that the *S. cerevisiae* OST does not discriminate between M_5GN_2-PP-Dol isomers. The M_5GN_2 glycopeptides synthesized by the *T. vaginalis* and *E. histolytica* OST also resembled the M_5GN_2-PP-Dol donor pool; hence, the OST from these organisms does not select biosynthetic M_5GN_2-PP-Dol in preference to other M_5GN_2-PP-Dol isomers (Fig. 3 D). M_5GN_2 glycopeptides synthesized by the *T. cruzi* OST were twofold deficient in biosynthetic M_5GN_2-NYT and enriched in one or more M_5GN_2-NYT isomers that have one α-1,2–linked mannose residue (Fig. 3 D). This result, taken together with a reduced transfer rate for $M_{3\text{-}6}GN_2$-PP-Dol relative to $M_{7\text{-}9}GN_2$-PP-Dol (Fig. 2 F) by the *T. cruzi* OST suggests that a terminal α-1,2–linked mannose residue on the B or C antennae of M_9GN_2-PP-Dol serves as a positive determinant for substrate selection by the *T. cruzi* OST.

Donor substrate competition experiments were conducted using purified biosynthetic M_5GN_2-PP-Dol (Fig. 3 A, isomer b), M_9GN_2-PP-Dol (Fig. 3 A, compound a), and $G_3M_9GN_2$-PP-Dol. The *T. vaginalis* OST will synthesize $G_3M_9GN_2$-NYT when $G_3M_9GN_2$-PP-Dol is the sole donor substrate (Fig. 4 A, profile a). The absence of the M_5GN_2-NYT product indicates that the endogenous donor substrate is not abundant in the assay mix relative to the exogenous donor substrate. Analogous results were obtained using detergent extracts prepared from *T. cruzi*, *E. histolytica*, and *C. neoformans* (unpublished data). When the M_5GN_2-PP-Dol/ $G_3M_9GN_2$-PP-Dol ratio is 2.5:1, the yeast OST primarily synthesized $G_3M_9GN_2$-NYT, unlike the *T. vaginalis* OST that synthesized M_5GN_2-NYT (Fig. 4 A, profiles b and c). Quantification of this competition experiment, as well as additional assays containing 1.5 μM M_5GN_2-PP-Dol and variable concentrations of $G_3M_9GN_2$-PP-Dol, showed that donor substrate selection by the *T. vaginalis* (Fig. 4 B, squares) and *S. cerevisiae* (Fig. 4 B, circles) OST occurs across a wide range of donor substrate ratios (Fig. 4 B). Additional donor substrate competition experiments were conducted using 1:1 mixtures of the three purified oligosaccharide donors (Fig. 4, C–E). The *S. cerevisiae* OST selects $G_3M_9GN_2$-PP-Dol in preference to both nonglucosylated donors (Fig. 4, C and D) but does not discriminate between M_5GN_2-PP-Dol and M_9GN_2-PP-Dol (Fig. 4 E). The OST from *E. histolytica* and *T. vaginalis* selects both nonglucosylated

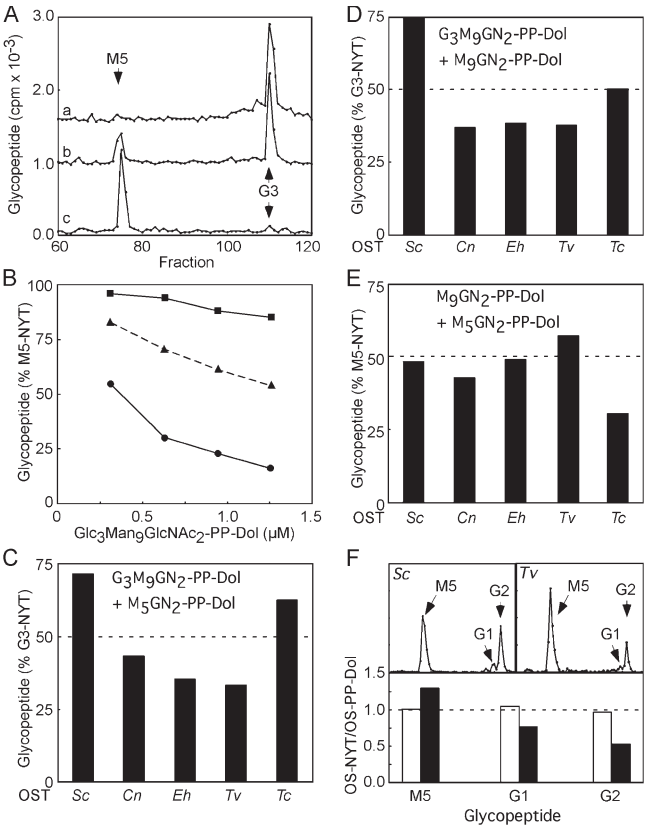

Figure 4. **Oligosaccharide donor competition assays.** OST activity was assayed using a constant concentration of the acceptor tripeptide (5 μM in A, B, and F and 10 μM in C–E). (A) Glycopeptide products from assays of the *T. vaginalis* (a and c) or *S. cerevisiae* (b) OST using 1 μM $G_3M_9GN_2$-PP-Dol (a) or 0.6 μM $G_3M_9GN_2$-PP-Dol plus 1.5 μM M_5GN_2-PP-Dol (b and c) were resolved by HPLC. For clarity, column profiles have been offset on the vertical axis. (B) The *T. vaginalis* (squares) or *S. cerevisiae* (circles) OST were assayed using 1.5 μM M_5GN_2-PP-Dol and increasing concentrations of $G_3M_9GN_2$-PP-Dol. Glycopeptide products were resolved by HPLC to determine the percentage of M_5GN_2-NYT. The dashed line indicates the composition (in percentage of M_5GN_2-PP-Dol) of the donor substrate mixtures. (C–E) Purified *S. cerevisiae* (*Sc*) or detergent extracts of *C. neoformans* (*Cn*), *E. histolytica* (*Eh*), *T. vaginalis* (*Tv*), or *T. cruzi* (*Tc*) membranes were assayed using the following donor substrate mixtures: 1 μM $G_3M_9GN_2$-PP-Dol + 1 μM M_5GN_2-PP-Dol (C), 1 μM $G_3M_9GN_2$-PP-Dol + 1 μM M_9GN_2-PP-Dol (D), and 1 μM M_9GN_2-PP-Dol + 1 μM M_5GN_2-PP-Dol (E). Glycopeptides were resolved by HPLC to determine product composition. (F) The *S. cerevisiae* and *T. vaginalis* OST were assayed using the following mixture: ($G_2M_9GN_2$-PP-Dol/$G_1M_9GN_2$-PP-Dol/M_9GN_2-PP-Dol/M_5GN_2-PP-Dol, 35:6:2:57). Glycopeptides were resolved by HPLC (top). The M_5GN_2-NYT (M5), $G_1M_9GN_2$-NYT (G1), and $G_2M_9GN_2$-NYT (G2) peaks are labeled. The *T. vaginalis* OST (closed bars), but not the yeast OST (open bars), shows reduced utilization of $G_2M_9GN_2$-PP-Dol and $G_1M_9GN_2$-PP-Dol relative to M_5GN_2-PP-Dol (bottom).

donors in preference to $G_3M_9GN_2$-PP-Dol (Fig. 4, C and D) but does not discriminate between M_5GN_2-PP-Dol and M_9GN_2-PP-Dol (Fig. 4 E). The *T. cruzi* OST does not discriminate between M_9GN_2-PP-Dol and $G_3M_9GN_2$-PP-Dol (Fig. 4 D), but both donors are selected in preference to M_5GN_2-PP-Dol (Fig. 4, C and E). In contrast, both the glucosylated donor and biosynthetic M_5GN_2-PP-Dol are nonoptimal donors for the *C. neoformans* OST relative to the in vivo donor (Fig. 4, D and E).

The observation that $G_3M_9GN_2$-PP-Dol but not M_9GN_2-PP-Dol is a nonoptimal donor for the *T. vaginalis* and *E. histolytica* OST suggests that the A antennae of M_5GN_2-PP-Dol may be recognized by the OST in these organisms. To test this hypothesis, an additional competition experiment was performed using a mixture of purified M_5GN_2-PP-Dol and an enriched sample of $G_2M_9GN_2$-PP-Dol. The $G_2M_9GN_2$-PP-Dol preparation contains $G_1M_9GN_2$-PP-Dol as a minor component. Glycopeptide products synthesized by the *S. cerevisiae* and *T. vaginalis* OST were resolved by HPLC (Fig. 4 F, top). The initial transfer rates of ~1 for the *S. cerevisiae* OST serves as an important control for the observed lower transfer rates of $G_2M_9GN_2$-PP-Dol and $G_1M_9GN_2$-PP-Dol relative to M_5GN_2-PP-Dol by the *T. vaginalis* OST. Each additional glucose residue on the A branch of the oligosaccharide reduces the normalized initial transfer rate by the *T. vaginalis* OST.

Kinetic parameters for the OS-PP-Dol donor

Enzyme kinetic experiments suggest that selection of the fully assembled OS-PP-Dol by the yeast or mammalian OST occurs by allosteric communication between a regulatory OS-PP-Dol binding site and the donor substrate binding site on STT3, in addition to oligosaccharide structure–dependent alterations in tripeptide substrate binding affinity (Karaoglu et al., 2001; Kelleher et al., 2003). Nonlinear Lineweaver-Burk plots for the OS-PP-Dol substrate are diagnostic of the cooperative OS-PP-Dol binding kinetics of the yeast and mammalian OST (Karaoglu et al., 2001). Donor substrate saturation experiments for the *T. vaginalis* (Fig. 5 A), *E. histolytica* (Fig. 5 C), and *T. cruzi* enzymes (Fig. 5 D) were conducted using a constant concentration of tripeptide acceptor and increasing concentrations of purified OS-PP-Dols. The linear Lineweaver-Burk plots yielded K_m values in the submicromolar range for the in vivo donor substrate. The experimental data for the *T. vaginalis* OST was replotted as an Eadie-Hofstee plot (Fig. 5 B). The linear Eadie-Hofstee plot for the *T. vaginalis* OST is inconsistent with cooperative OS-PP-Dol binding kinetics. In contrast, the *S. cerevisiae* OST binds the same donor substrate (M_5GN_2-PP-Dol) in a cooperative manner, as revealed by a nonlinear Eadie-Hofstee plot (Fig. 5 B, inset). Additional donor substrate saturation experiments using the nonoptimal donors (M_5GN_2-PP-Dol for *T. cruzi* OST and $G_3M_9GN_2$-PP-Dol for *T. vaginalis* OST) did not reveal differences in the apparent K_m that could account for the lower transfer rates of the nonoptimal donor substrate (unpublished data). Donor substrate selection by the protist OST does not involve a regulatory OS-PP-Dol binding site, nor is it explained by a reduced affinity for the nonoptimal oligosaccharide donor.

Kinetic parameters for the tripeptide substrate acceptor

Reduced transfer rates for nonoptimal donors by the yeast and mammalian OST is in part explained by a reduced binding affinity for the tripeptide acceptor in the presence of an OS-PP-Dol assembly intermediate (Breuer and Bause, 1995; Gibbs and Coward, 1999; Karaoglu et al., 2001; Kelleher et al., 2003). The *T. vaginalis* (Fig. 6 A) and *T. cruzi* (Fig. 6 B) OST were assayed in the presence of a constant concentration of the optimal and nonoptimal oligosaccharide donors and increasing concentrations

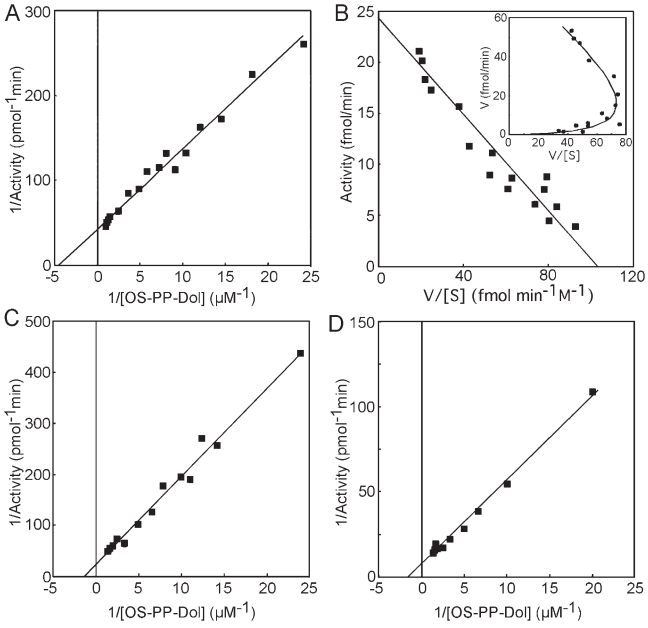

Figure 5. **Kinetic parameters for the oligosaccharide donor substrate.** OST activity was assayed using a constant concentration of the acceptor tripeptide substrate (10 μM in A, B, and D and 15 μM in C) and variable concentrations of M_5GN_2-PP-Dol (A–C) or M_9GN_2-PP-Dol (D). (A, C, and D) Lineweaver-Burk plots (1/OST activity versus 1/[OS-PP-Dol]) for the *T. vaginalis* (A; K_m = 0.22 μM), *E. histolytica* (C; K_m = 0.72 μM), or *T. cruzi* (D; K_m = 0.49 μM) OST were linear. (B) An Eadie-Hofstee plot (OST activity vs. OST activity/[OS-PP-Dol]) for the *T. vaginalis* (K_m = 0.19 μM) OST was linear. The inset shows an Eadie-Hofstee plot for the *S. cerevisiae* OST using M_5GN_2-PP-Dol as the donor substrate.

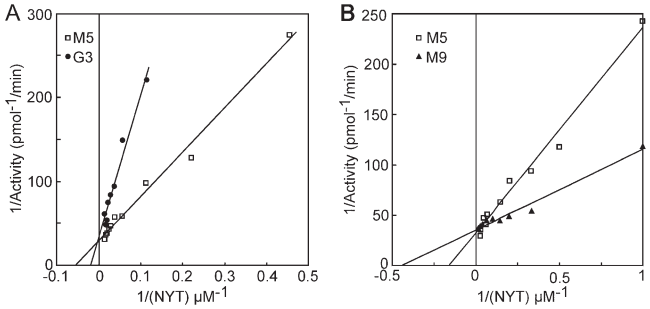

Figure 6. **Kinetic parameters for the tripeptide acceptor substrate.** OST activity was assayed using a constant concentration of the OS-PP-Dol donor (1 μM M_5GN_2-PP-Dol or $G_3M_9GN_2$-PP-Dol in A and 0.8 μM M_5GN_2-PP-Dol or M_9GN_2-PP-Dol in B) and increasing concentrations of acceptor tripeptide substrate. (A) Lineweaver-Burk plots for the *T. vaginalis* OST yielded apparent K_m values of 17 μM (M_5GN_2-PP-Dol donor) and 53 μM ($G_3M_9GN_2$-PP-Dol) for the acceptor tripeptide. (B) Lineweaver-Burk plots for the *T. cruzi* OST yielded apparent K_m values of 2.3 μM (M_9GN_2-PP-Dol donor) and 6.9 μM (M_5GN_2-PP-Dol) for the acceptor tripeptide.

of the tripeptide acceptor. The linear Lineweaver-Burk plots for the tripeptide acceptors were indicative of a single acceptor tripeptide binding site, as observed for the yeast and mammalian OST (Karaoglu et al., 2001; Kelleher et al., 2003). The nonoptimal donor substrate ($G_3M_9GN_2$-PP-Dol for *T. vaginalis* and M_5GN_2-PP-Dol for *T. cruzi*) reduces the binding affinity of the OST for the tripeptide acceptor. In both cases, the threefold decrease in acceptor tripeptide binding affinity is responsible for the reduction in the normalized transfer rate when the acceptor tripeptide is not saturating. The apparent V_{max} is not influenced by the structure of the OS-PP-Dol donor, as revealed by a shared I/V intercept, when the oligosaccharide donors are present in fourfold excess relative to the apparent K_m for the donor substrate (Fig. 6 A).

Discussion

Donor substrate selection of nonglucosylated oligosaccharides

GN_2-PP-Dol is the smallest oligosaccharide donor that is an effective substrate for the yeast OST (Sharma et al., 1981; Bause et al., 1995; Gibbs and Coward, 1999). The 2′ *N*-acetyl modification on the first saccharide is critical for catalysis, whereas the 2′ *N*-acetyl modification on the second residue is important for substrate recognition (Tai and Imperiali, 2001). Efficient *N*-glycosylation by the OST from higher eukaryotes is also dependent on the terminal glucose residue on the A antennae of the oligosaccharide (Turco et al., 1977; Trimble et al., 1980). As the OS-PP-Dol donors synthesized by many protists and the fungi *C. neoformans* lack glucose residues, one might predict that the OST from these organisms would only recognize the $GlcNAc_2$ core of the donor substrate. However, donor substrate competition experiments demonstrate that the in vivo oligosaccharide donor for *T. vaginalis*, *E. histolytica*, *T. cruzi*, and *C. neoformans* is a preferred substrate relative to certain larger and/or smaller OS-PP-Dol compounds. To our knowledge, this is the first evidence that oligosaccharide donor substrate selection is not restricted to organisms that synthesize the triglucosylated oligosaccharide donor. In all four cases, preferential utilization of the in vivo donor is less stringent than that observed for the *S. cerevisiae* or mammalian OST both in terms of the size range of compounds that are optimal in vitro substrates and the fold selection of the in vivo donor substrate relative to nonoptimal donors.

The predicted one-subunit OST from *T. cruzi* utilizes larger OS-PP-Dol compounds, including the in vivo donor M_9GN_2-PP-Dol in preference to M_5GN_2-PP-Dol. The latter compound is one of four lumenal OS-PP-Dol assembly intermediates that could compete in vivo with M_9GN_2-PP-Dol as a donor substrate. The observed two- to threefold more rapid in vitro transfer of M_9GN_2-PP-Dol than M_5GN_2-PP-Dol appears to be sufficient to ensure that small assembly intermediates are rarely used in vivo, in part because M_9GN_2-PP-Dol is more abundant in the *T. cruzi* ER than the luminally oriented ($M_{5\text{-}8}GN_2$-PP-Dol) assembly intermediates (Parodi and Quesada-Allue, 1982). The presence of a terminal α-1,2–linked mannose residue on the B or C antennae appears to be important for preferential utilization of M_9GN_2-PP-Dol by the *T. cruzi* OST, as revealed by the relative transfer rates of M_5GN_2-PP-Dol isomer classes (Fig. 3) and by the reduced utilization of $M_{3\text{-}6}GN_2$-PP-Dol relative to M_9GN_2-PP-Dol. In vivo transfer of an assembly intermediate may be deleterious, as protein-linked high-mannose oligosaccharides that lack the terminal mannose residue on the B antennae (M8B isomer) or C antennae (M8C isomer) are less efficiently glucosylated by the UDP-glucose glycoprotein

glucosyltransferase (UGGT; Trombetta and Parodi, 2003). UGGT, which was first detected in *T. cruzi*, serves as the folding sensor for the glycoprotein quality-control pathway in the ER (Caramelo et al., 2003).

The predicted four-subunit OSTs from *T. vaginalis* and *E. histolytica* (Fig. 1) transfer the in vivo donor (M_5GN_2-PP-Dol) at the same rate as other OS-PP-Dol compounds that lack glucose residues ($M_{4\text{-}9}GN_2$-PP-Dol), including M_5GN_2-PP-Dol isomers that lack one or more mannose residues on the A antennae. Because synthesis of the M_5GN_2-PP-Dol donor is completed on the cytoplasmic face of the rough ER, the *T. vaginalis* and *E. histolytica* OST do not need to discriminate between luminally oriented M_5GN_2-PP-Dol and cytoplasmically oriented OS-PP-Dol assembly intermediates. Consequently, M_5GN_2-NYT is the major glycopeptide synthesized in vitro when an acceptor tripeptide is incubated with intact *T. vaginalis* or *E. histolytica* membranes (Samuelson et al., 2005) despite the lack of a mechanism to discriminate against underassembled oligosaccharide donors. We propose that the STT3 active-site subunit of the OST has evolved to have a catalytic site that is optimal for the in vivo oligosaccharide. For *T. vaginalis*, *E. histolytica*, and *C. neoformans*, the proposed loss of genes that encode the ALG glucosyltransferases (ALG6, -8, and -10; Samuelson et al., 2005) has apparently been accompanied by compensatory alterations in the STT3 structure that are optimal for an oligosaccharide donor with an A antennae that lacks all three glucose residues.

The predicted seven-subunit *C. neoformans* OST transfers the larger mannosylated OS-PP-Dol donors ($M_{7\text{-}9}GN_2$-PP-Dol) more rapidly than smaller assembly intermediates or $G_3M_9GN_2$-PP-Dol. Utilization of the fully assembled in vivo donor in preference to luminally exposed OS-PP-Dol assembly intermediates may be a shared property of the OST in organisms that synthesize donors larger than M_5GN_2-PP-Dol. The relatively modest ($\sim$1.5-fold) preference for M_9GN_2-PP-Dol relative to biosynthetic M_5GN_2-PP-Dol leads to selective synthesis of M_9GN_2-NYT when the acceptor tripeptide is incubated with intact *C. neoformans* membranes (Samuelson et al., 2005).

Kinetic analysis of the *T. cruzi* and *T. vaginalis* OST revealed that oligosaccharide structure–mediated modulation of acceptor substrate binding affinity is a conserved property of the eukaryotic OST that can be ascribed to the STT3 active site. The threefold reduction in acceptor substrate binding affinity readily accounts for the reduced transfer of nonoptimal donors when the acceptor tripeptide is present at subsaturating levels. Future studies will address the order of substrate binding to the one- and four-subunit OSTs that are predicted for *T. cruzi* and *E. histolytica*. One objective of these experiments will be to determine whether the subunit composition of protist complexes matches the bioinformatic predictions.

Candidate subunits for the regulatory OS-PP-Dol binding site

Cooperative OS-PP-Dol binding by the *S. cerevisiae* OST is not explained by dimerization of heterooctamers, as coimmunoprecipitation experiments using yeast strains that express STT3-HA_3 and STT3-His_6FLAG_1 from chromosomal loci did not reveal higher order OST oligomers (Karaoglu et al., 2001). Potential explanations for the discrepancy between a recent report describing dimeric assembly of the yeast OST complex (Chavan et al., 2006) and our previous conclusions are being explored. Cooperative OS-PP-Dol binding is not explained by separate but interacting binding sites for the chitobiose core of $G_3M_9GN_2$-PP-Dol and the terminal glucose residue, because cooperative binding by the yeast or canine OST is not dependent on the presence of glucose residues on the oligosaccharide donor, as confirmed here using M_5GN_2-PP-Dol as a donor substrate. Instead, our results indicate that cooperative donor substrate binding is diagnostic of a regulatory OS-PP-Dol binding site that is primarily responsible for the highly selective utilization of the $G_3M_9GN_2$-PP-Dol donor (Karaoglu et al., 2001; Kelleher et al., 2003).

Based on a kinetic analysis of canine OST isoforms, we proposed that the regulatory OS-PP-Dol binding site is not located on the catalytic subunit (STT3A or -B), but is instead provided by one or more of the shared noncatalytic subunits. Support for this hypothesis has now been provided by recent experiments showing that a *T. cruzi* STT3 can assemble with the noncatalytic yeast OST subunits and, upon doing so, mediate selective utilization of $G_3M_9GN_2$-PP-Dol as the donor substrate both in vitro and in vivo (Castro et al., 2006).

One objective of this study was to determine whether protist OSTs use a regulatory OS-PP-Dol binding site to select the in vivo oligosaccharide donor. Unlike the *S. cerevisiae* and *Canis familiaris* OST, the predicted one-subunit OST from *T. cruzi* (STT3) and the predicted four-subunit OSTs from *E. histolytica* and *T. vaginalis* (STT3-OST1-OST2-WBP1) do not bind OS-PP-Dol in a cooperative manner; hence, the OST from these organisms lacks the regulatory OS-PP-Dol binding site. The simplest interpretation of this observation is that the regulatory OS-PP-Dol binding arose as additional subunits were acquired during evolution of the eukaryotic OST. The IAP and TUSC3 (N33) proteins dissociate from the canine OST during purification, so these OST3/OST6 family members are not candidates for the regulatory OS-PP-Dol binding site. OST4 and -5 can be discounted based on structural considerations because neither of these polypeptides has more than a few residues exposed to the lumen of the ER (Fig. 1). Therefore, cooperative OS-PP-Dol binding by the yeast or vertebrate OST correlates with the presence of a Swp1p/ribophorin II subunit in the OST complex. Extensive biochemical and genetic evidence supports direct interactions between Wbp1, Swp1p, and Ost2p (te Heesen et al., 1993; Silberstein et al., 1995), as well as between their respective mammalian homologues, OST48, ribophorin II, and DAD1 (Fu et al., 1997; Kelleher and Gilmore, 1997). We hypothesize that the regulatory OS-PP-Dol binding site is located on the Swp1p–Wbp1p–Ost2p subcomplex. Interestingly, OS-PP-Dol protects a critical cysteine residue in Wbp1p from modification by a cysteine-directed protein modification reagent (Pathak et al., 1995). A role for the Swp1p–Wbp1p–Ost2p subcomplex as the regulatory OS-PP-Dol binding site might help explain why expression of each of these subunits is essential for viability of *S. cerevisiae* (te Heesen et al., 1992, 1993; Silberstein et al., 1995). With the exception of *C. neoformans*,

there is a strong correlation between organisms that assemble a glucosylated oligosaccharide donor (either $G_3M_5GN_2$-PP-Dol or $G_3M_9GN_2$-PP-Dol) and organisms that express or are predicted to express a Swp1p/ribophorin II homologue (Samuelson et al., 2005; Kelleher and Gilmore, 2006).

Materials and methods

Preparation of detergent-extracted membranes and the *S. cerevisiae* OST

Trophozoites of *E. histolytica* strain HM1:IMSS were grown axenically (in the absence of bacteria or other cells) in TYI medium supplemented with 10% heat-inactivated adult bovine serum at 37°C. Axenic cultures of *T. vaginalis* strain G3 were maintained in TYM medium supplemented with 10% heat-inactivated horse serum at 37°C. Axenic cultures of *T. cruzi* epimastigotes (strain Y) were grown in the LIT medium supplemented with hemin and 10% heat-inactivated fetal calf serum at 25°C. *C. neoformans* strain B3501, maintained on YPD plates, was grown in YPD broth for 20 h at 30°C.

Whole cells were collected by centrifugation and resuspended in 10 mM Hepes, pH 7.4, 25 mM NaCl, 10 mM $MgCl_2$, and 1× protease inhibitor cocktail (PIC; as defined by Kelleher et al., 1992). *E. histolytica*, *T. vaginalis*, or *T. cruzi* cells were homogenized using 50 strokes of a Teflon-glass homogenizer. The *C. neoformans* cell suspension was mixed with an equal volume of glass beads and vortexed extensively (200 5-s bursts). Total membrane fractions were collected by a 30-min centrifugation of the cell homogenate at 267,000 g_{av} using a rotor (TLA 100.4; Beckman Coulter). The membrane pellets were solubilized in 1.5% digitonin, 20 mM Tris-Cl, pH 7.5, 500 mM NaCl, 1 mM $MgCl_2$, 1 mM $MnCl_2$, 1 mM DTT, and 1× PIC at a membrane concentration of 2 eq/μl (1 eq/μl = 50 A_{280} in 1% SDS). The detergent extracts were clarified by a 5-min centrifugation at 66,600 g_{av} using the rotor. The *S. cerevisiae* OST was purified from an epitope-tagged (6xHisFLAG-OST1) yeast strain as described previously (Karaoglu et al., 2001).

OST assays

Detergent extracts of the *E. histolytica*, *T. vaginalis*, *T. cruzi*, and *C. neo formans* membranes were diluted fourfold with 20 mM Tris-Cl, pH 7.4, 1 mM $MgCl_2$, 1 mM $MnCl_2$, 1 mM DTT, and 1× PIC. 5-μl aliquots of the 4×-diluted soluble extracts were assayed for OST activity in a total volume of 100 μl as described previously (Kelleher and Gilmore, 1997), using Nα-Ac-Asn-[^{125}I]Tyr-Thr-NH_2 as the acceptor substrate and either structurally homogeneous OS-PP-Dol compounds or a previously described heterogeneous bovine pancreas OS-PP-Dol pool (Kelleher et al., 2001) as the donor substrate. OST assays were supplemented with 1.4 mM deoxynojirimycin, 1.4 mM mannojirimycin, and 1.4 mM swainsonine to inhibit glucosidases and mannosidases. Glycopeptide products from OST assays were isolated with ConA Sepharose and quantified by gamma counting.

Structurally homogeneous $G_3M_9GN_2$-PP-Dol, M_9GN_2-PP-Dol, M_5GN_2-PP-Dol, and an enriched $G_2M_9GN_2$-PP-Dol preparation were purified as described previously (Kelleher et al., 2001) from porcine pancreas ($G_3M_9GN_2$-PP-Dol and $G_2M_9GN_2$-PP-Dol), an *alg5Δ* yeast strain (M_9GN_2-PP-Dol), or an *alg3Δ* yeast strain (M_5GN_2-PP-Dol).

The concentration and composition of OS-PP-Dol samples was determined from the yield and oligosaccharide distribution of radiolabeled glycopeptides obtained in the OST endpoint assay (Kelleher et al., 2001). In brief, 12–15 pmol of OS-PP-Dol was incubated with 60 fmol of purified yeast OST for 24–48 h under OST assay conditions to quantitatively convert the donor substrate into glycopeptides. The previously isolated heterogeneous bovine pancreas OS-PP-Dol pool consists of a mixture of biosynthetic OS-PP-Dol assembly intermediates and OS-PP-Dol degradation products that were produced by exposure of the OS-PP-Dol to endogenous mannosidases and glycosidases during isolation (Kelleher et al. 2001). As shown in Fig. S1 B, the bovine OS-PP-Dol pool has the following oligosaccharide composition: 4.7% M_3GN_2, 14% M_4GN_2, 19% M_5GN_2, 23% M_6GN_2,17% M_7GN_2, 11% M_8GN_2, 3.7% M_9GN_2, 1% $G_1M_9GN_2$, 1.5% $G_2M_9GN_2$, and 5.1% $G_3M_9GN_2$. Because of low abundance in the donor pool, initial transfer rates are not reported for $G_1M_9GN_2$-PP-Dol and $G_2M_9GN_2$-PP-Dol.

Assays designed to analyze the donor substrate preference of the OST using the bovine OS-PP-Dol library contained 1.2 μM OS-PP-Dol and were terminated before 3% of the total donor was consumed. Donor substrate competition experiments using purified donors were terminated before 10% of the substrate was consumed. Glycopeptide products from the competition experiments were eluted from the ConA beads and resolved according to oligosaccharide size by HPLC as described previously (Mellis and Baenziger, 1981; Kelleher et al., 2001), except that the HPLC buffer A was acetonitrile/water/acetic acid/triethlyamine (73.6:23:2.4:1), whereas HPLC buffer B was water/acetic acid/triethlyamine (91:3:6). Glycopeptides prepared using the yeast OST and purified OS-PP-Dol compounds served as HPLC elution standards.

Digestions of M_5GN_2-NYT with α-1,2 mannosidase

OST assays to prepare M_5GN_2 glycopeptides using the heterogeneous OS-PP-Dol library were designed to ensure that <10% of the total M_5GN_2-PP-Dol was converted to M_5GN_2-NYT. HPLC fractions corresponding to M_5GN_2-NYT were dried and resuspended in 50 μl of 1× reaction buffer supplied by the manufacturer (Prozyme) and incubated for 18 h at 37°C with 0.33 mU α-1,2 mannosidase. The Savant-dried glycopeptide digestion products were dissolved in 500 μl HPLC buffer A and resolved by HPLC as described in the preceeding paragraph.

Analysis of kinetic data

The kinetic parameters for the tripeptide acceptor and oligosaccharide donor for the *T. vaginalis*, *T. cruzi*, and *E. histolytica* enzymes were determined by a nonlinear least-squares fit of the kinetic data to the Michaelis-Menten equation and by linear least-squares fits of Lineweaver-Burk plots or Eadie-Hofstee plots. The kinetic parameters for the dolichol-oligosaccharide donor for the *S. cerevisiae* enzyme were obtained using a nonlinear least-squares fit of the kinetic data to equations for a substrate activated enzyme as described previously (Karaoglu et al., 2001). Kaleidagraph 3.5 (Synergy Software) was used for curve fitting.

Online supplemental material

Fig. S1 shows the oligosaccharide composition analysis of the OS-PP-Dol library used for the experiments in Fig. 2 and Fig. 3. Online supplemental material is available at http://www.jcb.org/cgi/content/full/jcb.200611079/DC1.

The authors thank Phillips Robbins for helpful discussions.

This work was supported by National Institutes of Health grants GM43768 (R. Gilmore), AI44070 (J. Samuelson), and GM31318 (Phillips Robbins).

Submitted: 15 November 2006
Accepted: 5 March 2007

References

Bause, E., W. Breuer, and S. Peters. 1995. Investigation of the active site of oligosaccharyltransferase from pig liver using synthetic tripeptides as tools. *Biochem. J.* 312:979–985.

Bosch, M., S. Trombetta, U. Engstrom, and A.J. Parodi. 1988. Characterization of dolichol diphosphate oligosaccharide: protein oligosaccharyltransferase and glycoprotein-processing glucosidases occurring in trypanosomatid protozoa. *J. Biol. Chem.* 263:17360–17365.

Breuer, W., and E. Bause. 1995. Oligosaccharyl transferase is a constitutive component of an oligomeric protein complex from pig liver endoplasmic reticulum. *Eur. J. Biochem.* 228:689–696.

Burda, P., and M. Aebi. 1999. The dolichol pathway of N-linked glycosylation. *Biochim. Biophys. Acta.* 1426:239–257.

Caramelo, J.J., O.A. Castro, L.G. Alonso, G. De Prat-Gay, and A.J. Parodi. 2003. UDP-Glc:glycoprotein glucosyltransferase recognizes structured and solvent accessible hydrophobic patches in molten globule-like folding intermediates. *Proc. Natl. Acad. Sci. USA.* 100:86–91.

Castro, O., F. Movsichoff, and A.J. Parodi. 2006. Preferential transfer of the complete glycan is determined by the oligosaccharyltransferase complex and not by the catalytic subunit. *Proc. Natl. Acad. Sci. USA.* 103:14756–14760.

Chavan, M., Z. Chen, G. Li, H. Schindelin, W.J. Lennarz, and H. Li. 2006. Dimeric organization of the yeast oligosaccharyl transferase complex. *Proc. Natl. Acad. Sci. USA.* 103:8947–8952.

de la Canal, L., and A.J. Parodi. 1987. Synthesis of dolichol derivatives in trypanosomatids. Characterization of enzymatic patterns. *J. Biol. Chem.* 262:11128–11133.

Freeze, H.H., and M. Aebi. 2005. Altered glycan structures: the molecular basis of congenital disorders of glycosylation. *Curr. Opin. Struct. Biol.* 15:490–498.

Fu, J., M. Ren, and G. Kreibich. 1997. Interactions among subunits of the oligosaccharyltransferase complex. *J. Biol. Chem.* 272:29687–29692.

Gavel, Y., and G. Von Heijne. 1990. Sequence differences between glycosylated and non-glycosylated Asn-X-Thr/Ser acceptor sites: implications for protein engineering. *Protein Eng.* 3:433–442.

Gibbs, B.S., and J.K. Coward. 1999. Dolichylpyrophosphate oligosaccharides: large scale isolation and evaluation as oligosaccharyltransferase substrates. *Bioorg. Med. Chem.* 7:441–447.

Helenius, A., and M. Aebi. 2004. Roles of N-linked glycans in the endoplasmic reticulum. *Annu. Rev. Biochem.* 73:1019–1049.

Helenius, J., D.T. Ng, C.L. Marolda, P. Walter, M.A. Valvano, and M. Aebi. 2002. Translocation of lipid-linked oligosaccharides across the ER membrane requires Rft1 protein. *Nature.* 415:447–450.

Karaoglu, D., D.J. Kelleher, and R. Gilmore. 1997. The highly conserved Stt3 protein is a subunit of the yeast oligosaccharyltransferase and forms a subcomplex with Ost3p and Ost4p. *J. Biol. Chem.* 272:32513–32520.

Karaoglu, D., D.J. Kelleher, and R. Gilmore. 2001. Allosteric regulation provides a molecular mechanism for preferential utilization of the fully assembled dolichol-linked oligosaccharide by the yeast oligosaccharyltransferase. *Biochemistry.* 40:12193–12206.

Kelleher, D.J., and R. Gilmore. 1997. DAD1, the defender against apoptotic cell death, is a subunit of the mammalian oligosaccharyltransferase. *Proc. Natl. Acad. Sci. USA.* 94:4994–4999.

Kelleher, D.J., and R. Gilmore. 2006. An evolving view of the eukaryotic oligosaccharyltransferase. *Glycobiology.* 16:47R–62R.

Kelleher, D.J., G. Kreibich, and R. Gilmore. 1992. Oligosaccharyltransferase activity is associated with a protein complex composed of ribophorins I and II and a 48 kD protein. *Cell.* 69:55–65.

Kelleher, D.J., D. Karaoglu, and R. Gilmore. 2001. Large-scale isolation of dolichol-linked oligosaccharides with homogeneous oligosaccharide structures: determination of steady-state dolichol-linked oligosaccharide compositions. *Glycobiology.* 11:321–333.

Kelleher, D.J., D. Karaoglu, E.C. Mandon, and R. Gilmore. 2003. Oligosacchar yltransferase isoforms that contain different catalytic STT3 subunits have distinct enzymatic properties. *Mol. Cell.* 12:101–111.

Koiwa, H., F. Li, M.G. McCully, I. Mendoza, N. Koizumi, Y. Manabe, Y. Nakagawa, J. Zhu, A. Rus, J.M. Pardo, et al. 2003. The STT3a subunit isoform of the *Arabidopsis* oligosaccharyltransferase controls adaptive responses to salt/osmotic stress. *Plant Cell.* 15:2273–2284.

Mellis, S.J., and J.U. Baenziger. 1981. Separation of neutral oligosaccharides by high-performance liquid chromatography. *Anal. Biochem.* 114:276–280.

Nilsson, I., D.J. Kelleher, Y. Miao, Y. Shao, G. Kreibich, R. Gilmore, G. Von Heijne, and A.E. Johnson. 2003. Photocross-linking of nascent chains to the STT3 subunit of the oligosaccharyltransferase complex. *J. Cell Biol.* 161:715–725.

Parodi, A.J. 1993. N-glycosylation in trypanosomatid protozoa. *Glycobiology.* 3:193–199.

Parodi, A.J., and L.A. Quesada-Allue. 1982. Protein glycosylation in *Trypanosoma cruzi*. I. Characterization of dolichol-bound monosaccharides and oligosaccharides synthesized "in vivo". *J. Biol. Chem.* 257:7637–7640.

Pathak, R., T.L. Hendrickson, and B. Imperiali. 1995. Sulfhydryl modification of the yeast Wbp1p inhibits oligosaccharyl transferase activity. *Biochemistry.* 34:4179–4185.

Samuelson, J., S. Banerjee, P. Magnelli, J. Cui, D.J. Kelleher, R. Gilmore, and P.W. Robbins. 2005. The diversity of dolichol-linked precursors to Asn-linked glycans likely results from secondary loss of sets of glycosyltransferases. *Proc. Natl. Acad. Sci. USA.* 102:1548–1553.

Sharma, C.B., L. Lehle, and W. Tanner. 1981. N-glycosylation of yeast proteins. Characterization of the solubilized oligosaccharyltransferase. *Eur. J. Biochem.* 116:101–108.

Silberstein, S., P.G. Collins, D.J. Kelleher, and R. Gilmore. 1995. The essential OST2 gene encodes the 16-kD subunit of the yeast oligosaccharyltransferase, a highly conserved protein expressed in diverse eukaryotic organisms. *J. Cell Biol.* 131:371–383.

Spirig, U., M. Glavas, D. Bodmer, G. Reiss, P. Burda, V. Lippuner, S. te Heesen, and M. Aebi. 1997. The STT3 protein is a component of the yeast oligosaccharyltransferase complex. *Mol. Gen. Genet.* 256:628–637.

Tai, V.W., and B. Imperiali. 2001. Substrate specificity of the glycosyl donor for oligosaccharyl transferase. *J. Org. Chem.* 66:6217–6228.

te Heesen, S., B. Janetzky, L. Lehle, and M. Aebi. 1992. The yeast WBP1 is essential for oligosaccharyltransferase activity in vivo and in vitro. *EMBO J.* 11:2071–2075.

te Heesen, S., R. Knauer, L. Lehle, and M. Aebi. 1993. Yeast Wbp1p and Swp1p form a protein complex essential for oligosaccharyl transferase activity. *EMBO J.* 12:279–284.

Trimble, R.B., J.C. Byrd, and F. Maley. 1980. Effect of glucosylation of lipid intermediates on oligosaccharide transfer in solubilized microsomes from *Saccharomyces cerevisiae*. *J. Biol. Chem.* 255:11892–11895.

Trombetta, E.S., and A.J. Parodi. 2003. Quality control and protein folding in the secretory pathway. *Annu. Rev. Cell Dev. Biol.* 19:649–676.

Turco, S.J., B. Stetson, and P.W. Robbins. 1977. Comparative rates of transfer of lipid-linked oligosaccharides to endogenous glycoprotein acceptors in vitro. *Proc. Natl. Acad. Sci. USA.* 74:4411–4414.

Yan, Q., and W.J. Lennarz. 2002. Studies on the function of the oligosaccharyltransferase subunits: Stt3p is directly involved in the glycosylation process. *J. Biol. Chem.* 277:47692–47700.